PREPARATION OF SUPPORTED NANOPARTICLES USING SUPERCRITICAL FLUIDS

Y. Zhang and C. Erkey*
Department of Chemical Engineering
University of Connecticut
Storrs, CT 06269
e-mail: cerkey@engr.uconn.edu
fax: (860) 486 - 2959

Platinum and ruthenium nanoparticles supported on carbon aerogel, carbon black, silica aerogel, silica and γ-alumina substrates, were synthesized via a supercritical fluid route. Organometallic precursor, either dimethyl(1,5-cyclooctadiene)platinum (II) ($PtMe_2COD$) or bis(2,2,6,6-tetramethyl-3,5-heptanedionato)(1,5-cyclooctadiene) ruthenium (II) ($Ru(cod)(tmhd)_2$), was dissolved in supercritical carbon dioxide ($scCO_2$) and impregnated into the porous substrates. After depressurization, the impregnated organometallic precursors were converted to metal particles at a predetermined temperature in the presence of nitrogen gas. The resulting nanocomposites were investigated by transmission electron microscopy (TEM) which revealed uniformly dispersed metal particles on each of the substrates with average particle sizes ranging from 1.2 nm to 6.4 nm and a narrow particle size distribution. A comparison of nanocomposites produced under different conditions showed that both the metal contents and particle sizes are controllable.

INTRODUCTION

Supported metal nanocomposites have unique electronic, optical, electro-optical, electrochemical, and catalytic properties that are directly related to the specific concentration, size and distribution of the metal particles within their host environment [1]. There are several ways to synthesize supported nanoparticles, including impregnation, deposition-precipitation, chemical vapor impregnation, sol-gel, or microemulsion using organic stabilizing agents. However, control over particle size, distribution, and metal concentration in the composite is challenging. Here we utilize a supercritical fluid as a processing medium to incorporate metal nanoparticles into different substrates [2].

EXPERIMENTAL

Carbon aerogel substrates with an average pore size of 20 nm were manufactured in-house. The details of the synthesis route for these CAs are described elsewhere [3]. Carbon black powder (Vulcan XC-72R) was purchased from Cabot, International. The silica aerogel (random 0.2 to 2.0 cm pieces) was purchased from MarkeTech International, Inc. Both silica and γ-alumina pellets were donated by Saint-Gobain NorPro, Inc. All of the chemicals were used as received except for the γ-Al_2O_3 which was dried at 300^{o}C for 2 hours.

A schematic diagram of the setup used for impregnation is given in Figure 1. The 54 ml vessel is custom manufactured from stainless steel and is fitted with two sapphire windows (1" ID, Sapphire Engineering, Inc.), poly-ether-ether-ketone o-rings (Valco Instruments, Inc.), a T-type thermocouple assembly (Omega Engineering, DP41-TC-MDSS), a pressure transducer (Omega Engineering, PX300-7.5KGV), a vent line, and a rupture disk assembly (Autoclave Engineers).

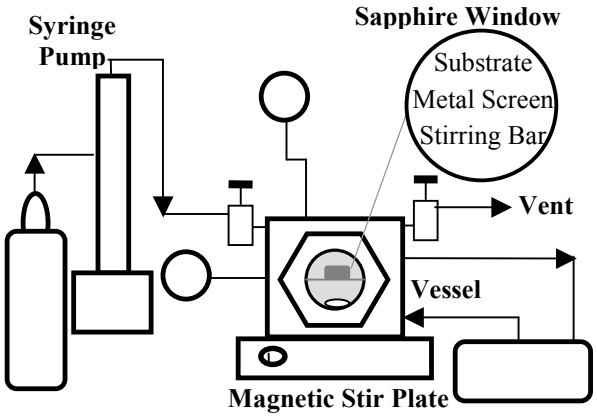

Figure 1 Schematic diagram for supercritical impregnation.

For each run, a certain amount of organometallic precursor, $PtMe_2COD$ or $Ru(cod)(tmhd)_2$, a stirring bar, and a certain amount of substrate were placed into the vessel. A stainless steel screen was used to separate the substrate from the stirring bar. The vessel was sealed and heated to 80°C by a circulating heater/cooler (Fischer Scientific Isotemp Refrigerated Circulator Model 90) via a machined internal coil. It was then charged slowly with CO_2 from a syringe pump (ISCO, 260D) up to a pressure of 27.6 MPa and kept at these conditions for 24 hours. During this process, all precursor put into the vessel was dissolved in $scCO_2$ or adsorbed into the substrate. The vessel was then depressurized slowly (0.46 MPa/min) through a restrictor into the atmosphere. After the vessel was cooled down, the precursor/substrate composite was taken out. The amount of the precursor adsorbed was determined by the weight change of the substrate using an analytical balance (Adventure Model AR2140) accurate to ±0.1 mg. Subsequently, the precursor/substrate composite was placed in an alumina process tube (Cole-Parmer) with dimensions of 25 mm (ID) x 28 mm (OD) x 1219.2 mm (L) and the tube was placed into a tube furnace (Model F1125 Thermolyne). The impregnated organometallic precursor was reduced thermally at predetermined temperatures in the presence of nitrogen gas with a flow rate of 100 cm^3min^{-1} for six hours. TGA of pure organometallic precursors and of precursor-substrate composites under a nitrogen atmosphere were used to select the minimum thermal reduction temperatures.

RESULTS AND DISCUSSION

The detailed preparation conditions and characterization results of the nanocomposites are listed in Table 1.

Table 1. Substrates, preparation conditions and metal particle sizes (measured by TEM)

	Me	Substrates		Reduction	Amounts Before Impregnation (g)		Composite Weight After Impregnation (g)	Metal Loading wt%	Average Particle Size (nm)
			Surface Area ($m^2 g^{-1}$)	Temp. (^oC)	*Substrate*	*Precursor*			
1	Ru	*CA*	*629*	*1000*	*0.205*	*0.406*	*0.303*	*7.7*	*3.8*
2	Ru	*CA*		*400*	*0.601*	*0.602*	*0.902*	*8.0*	*1.8*
3	Pt	*CA*		*300*	*0.722*	*1.852*	*1.660*	*40.0*	*3.0*
4	Ru	*SA*	*800*	*400*	*0.300*	*0.164*	*0.325*	*2.0*	*4.0*
5	Pt	*SA*		*300*	*0.843*	*0.375*	*1.059*	*12.0*	*3.9*
6	Pt	*CB*	*290*	*200*	*0.331*	*0.175*	*0.441*	*16.2*	*2.0*
7	Pt	Al_2O_3	*260*	*300*	*0.419*	*0.116*	*0.514*	*11.6*	*2.7*
8	Pt	Al_2O_3		*300*	*1.056*	*0.065*	*1.115*	*3.0*	*1.2*
9	Pt	SiO_2	*120*	*300*	*0.461*	*0.128*	*0.544*	*9.5*	*6.4*
10	Pt	SiO_2		*300*	*7.036*	*0.749*	*7.687*	*5.1*	*4.6*

Figure 2(a) is a TEM micrograph obtained from carbon aerogel supported ruthenium nanoparticles wherein the Ru nanoparticles appear as uniformly-dispersed circular dark features against the background contrast from the aerogel support with no evidence for any nanoparticle coalescence. The character of these nanoparticles was confirmed using EDXS and an example of a typical spectrum is shown in figure 2(b). The spectrum contains strong characteristic C and Ru X-ray peaks as expected, together with additional peaks corresponding to O and Cu. These latter peaks are artifacts which arise from adsorbed O and the Cu grid on which the TEM sample is supported, respectively. No lattice fringes were observed in images from most of the nanoparticles, presumably due to their small sizes and random orientations. Such fringes were, however, observed in occasional images and one example is shown in figure 2(a) inset image. The spacing is 2.3 Å which corresponds to the $\{10\bar{1}0\}$ planes of hexagonal-close packed metallic Ru. No evidence for grain boundaries or lattice defects was observed in such images, i.e. the individual Ru nanoparticles are defect-free single crystals. The Ru nanoparticles exhibit a narrow size distribution with particle sizes ranging from 2.8 to 4.3 nm with a mean value of 3.8 nm and a standard deviation of 0.5 nm.

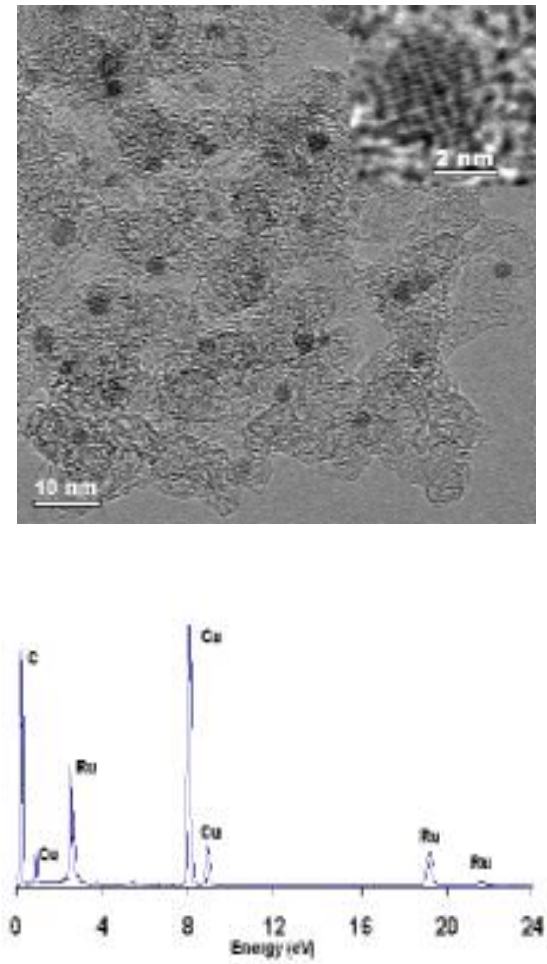

(2b)

Figure 2. TEM data obtained from sample 2. (a) HRTEM image of uniformly dispersed Ru nanoparticles on CA, the inset shows $\{10\bar{1}0\}$ lattice fringes in one Ru nanoparticle (inset); (b) corresponding EDXS spectrum.

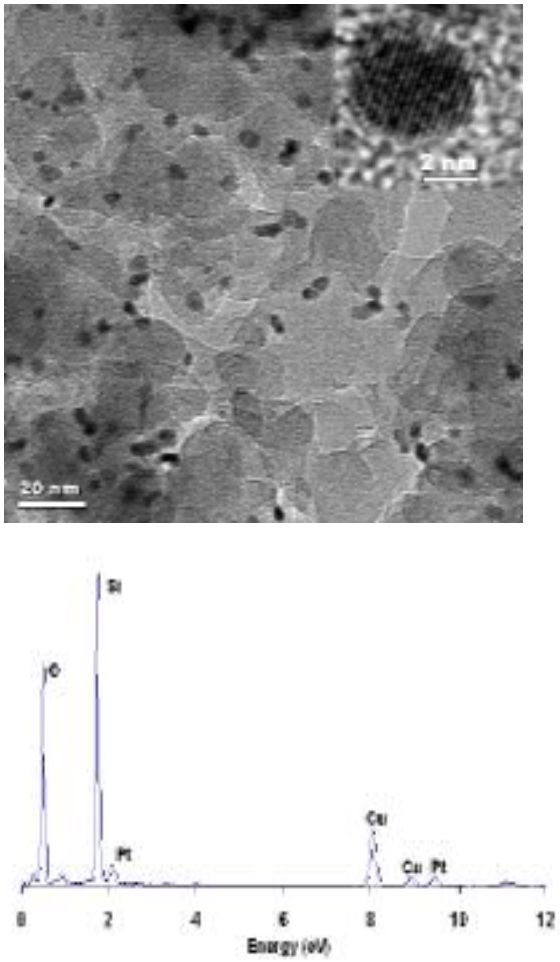

(3b)

Figure 3. TEM data obtained from sample 10. (a) HRTEM image of uniformly dispersed Pt nanoparticles on Silica, the inset shows {111} lattice fringes in one Pt nanoparticle (inset); (b) corresponding EDXS spectrum

Figure 3 shows the TEM data for silica supported Pt nanoparticles. Figure 3(a) reveals the morphology of Pt-loaded silica. Slightly ellipsoidal Pt nanoparticles are dispersed either on the surface of a silica crystallite or sandwiched between crystallites. Here again, no coalescence of the metal nanoparticles was observed. The inset image shows a single nanoparticle with 2.4 A lattice fringes corresponding to the {111} planes of face-centred cubic metallic Pt. Compared to sample 1, the Pt nanoparticles exhibit a slightly broader size distribution ranging from 2.3 to 6.8 nm with a mean particle size of 4.6 nm and a standard deviation of 1.6 nm. Figure 3(b) shows the corresponding EDXS spectrum which contains strong characteristic Si, O and Pt X-ray peaks, together with Cu peaks from the support grid.

Examples of typical TEM micrographs obtained from the other samples reveal uniformly dispersed metal nanoparticles with a mean particle size of 1.2 nm to 6.4 nm and a narrow particle size distribution. Comparison of the micrographs obtained from samples 7 and 8, as

well as samples 9 and 10, show that higher metal loadings result in larger particle sizes and broader distributions. This is not unexpected since a higher metal loading results in a larger number of nanoparticles per unit area and thus leads to a higher incidence of nanoparticle coalescence. Increasing the temperature at which the organometallic precursor is reduced also results in composites with larger particles and broader particle size distributions as shown by a comparison of samples 1 and 2. This may correspond to an increase in the mobility of the individual ruthenium or platinum nanoparticles, and hence to an increased incidence of nanoparticle coalescence.

CONCLUSIONS

This study demonstrated that the supercritical fluid route is an effective way to incorporate metal nanoparticles into different porous materials. Uniformly dispersed platinum and ruthenium nanoparticles with mean sizes of between 1.2 nm (3% Pt/ γ-Al_2O_3) and 6.4 nm (10% Pt/SiO_2) were obtained. The particle size and can be controlled to a certain extent by the metal loading in the composites, and by the temperature at which the organometallic precursors are converted to metal crystallites. The mean particle size and the size distribution are governed by the interaction between the organometallic precursors and the substrates. It was also shown that Ru(cod)$(tmhd)_2$ is an effective precursor for the preparation of supported Ru nanoparticles via the supercritical fluid route.

ACKNOWLEDGEMENTS

We gratefully acknowledge the financial support of US Army CECOM.

REFERENCES

[1] STAKHEEV, A. Y., KUSTOV, L. M. Appl. Catal. A, Vol. 188, **1999**, p. 3.

[2] MORLEY, S.K., MARR, P.C. WEBB, P.B., BERRY, A.R., ALLISON, F.J., MOLDOVAN, G., BROWN, P.D., HOWDLE, S.M., J. Mater. Chem., Vol. 12, **2002**, p. 1898

[3] SAQUING, C.D., CHENG, T.T., AINDOW, M., ERKEY, C., J. Phys. Chem. B., Vol. 108, **2004**, p. 7716.